

# Wear and corrosion resistant properties of electrodeposited Ni composite coating containing $\text{Al}_2\text{O}_3$ – $\text{TiO}_2$ composite powder

S. T. Aruna\* and G. Srinivas

Electrodeposited Ni composite coatings containing ceramic particles have been widely investigated due to their improved mechanical, wear and corrosion resistant properties over plain nickel coatings. The application of one of the most widely studied plasma spray powder,  $\text{Al}_2\text{O}_3$ –13 wt-% $\text{TiO}_2$ , has not been explored in electrodeposited nickel composites. In the present study, Ni/ $\text{Al}_2\text{O}_3$ –13 wt-% $\text{TiO}_2$  coatings have been electrodeposited using physically mixed commercial  $\text{Al}_2\text{O}_3$  and  $\text{TiO}_2$  powders. The microhardness, wear and corrosion resistant properties of the coatings have been investigated. It was found that the area fraction of particles incorporated in the nickel matrix was very high at lower current density, and the corresponding composite coating exhibited a maximum microhardness (~580 HK). Interestingly, corrosion resistance of Ni/ $\text{Al}_2\text{O}_3$ –13 wt-% $\text{TiO}_2$  composite coating was similar to that reported for Ni/ $\text{TiO}_2$ . The wear behaviour of Ni/ $\text{Al}_2\text{O}_3$ –13 wt-% $\text{TiO}_2$  coating was in between Ni/ $\text{Al}_2\text{O}_3$  and Ni/ $\text{TiO}_2$  coatings and thus exhibited a synergistic effect of the properties of  $\text{Al}_2\text{O}_3$  and  $\text{TiO}_2$  powders.

**Keywords:** Metal matrix composites, Wear, Corrosion, Microstructure, Electrochemical impedance spectroscopy, Particle size

## Introduction

Surface engineering techniques like electroplating, thermal spray, physical vapour deposition, etc., play a key role in enhancing the mechanical and tribological properties of various mechanical components used in various applications.<sup>1,2</sup> Electrodeposited metal matrix coatings are being developed to meet the particular demands of low friction coefficient and high wear resistance for current advanced technological applications, such as aerospace, defense, automobile and nuclear power industries. Electroplating of composite coating involves the codeposition of metallic, non-metallic or polymer particles with metal to improve the coating properties such as corrosion resistance, hardness and wear performance.<sup>3</sup> This method has the advantages like low cost, low temperature and single step process without additional thermal treatment.<sup>3</sup> Numerous nickel matrix composite coatings have been electrodeposited from different electrolyte baths containing nano/micrometre sized inert particles such as  $\text{TiO}_2$ , SiC,  $\text{CeO}_2$ ,  $\text{Al}_2\text{O}_3$ , TiC,  $\text{ZrO}_2$ , etc.<sup>4–11</sup>

In recent years, many papers have been published on the properties of electrodeposited Ni/ $\text{TiO}_2$  and Ni/ $\text{Al}_2\text{O}_3$  composite coatings.<sup>12–19</sup> Sun and Li reported decreased wear rate and coefficient of friction for Ni/ $\text{TiO}_2$  coatings

with increase in titania nanoparticle content.<sup>14</sup> Szczygiel and Kolodziej<sup>17</sup> have studied the corrosion resistance of Ni/ $\text{Al}_2\text{O}_3$  coatings in NaCl solution. Feng *et al.*<sup>18</sup> reported an improved wear resistance for nanostructured Ni/ $\text{Al}_2\text{O}_3$  composite coatings deposited under the influence of an external high magnetic field (8 T). The synthesis and properties of electrodeposited Ni/ $\text{Al}_2\text{O}_3$  and Ni/ $\text{TiO}_2$  composites have been widely studied, and seldom are there any reports on the synergistic effect of  $\text{Al}_2\text{O}_3$  and  $\text{TiO}_2$  particles on the properties of nickel composite coating.

$\text{Al}_2\text{O}_3$ –13 wt-% $\text{TiO}_2$  (AT) is one of the most widely studied plasma sprayed oxide coating because of its wear, corrosion and erosion resistance.<sup>19</sup> It is used as a wear resistant coating for machine components and also to improve the wear, corrosion and erosion resistances of steels.<sup>19,20</sup>

The present work is aimed at the preparation of electrodeposited Ni/AT composite coating and evaluation of its mechanical, wear and corrosion resistant properties. The obtained properties of Ni/AT composite coating are compared with the reported wear and corrosion resistant properties of Ni/ $\text{Al}_2\text{O}_3$  and Ni/ $\text{TiO}_2$  coatings.

## Experimental

Commercial titania (Sd. Fine Chemicals) and alumina (Alcoa) powders with average agglomerated particle sizes of 1.7 and 2  $\mu\text{m}$  respectively were used.  $\text{Al}_2\text{O}_3$ –13 wt-% $\text{TiO}_2$  (AT) powder was obtained by physically

Surface Engineering Division, Council of Scientific and Industrial Research-National Aerospace Laboratories, HAL Airport Road, Bangalore 560017, India

\*Corresponding author, email aruna\_reddy@nal.res.in

mixing 87 g of  $\text{Al}_2\text{O}_3$  and 13 g of  $\text{TiO}_2$  powders in a roller mill for 2 h without using any grinding media to ensure proper mixing without any further size reduction.

The above physically mixed powder was characterised for phase identification using a powder X-ray diffractometer (XRD) (Bruker D-8 Advance) with  $\text{Cu } K_\alpha$  radiation. The morphology of the powders was determined by field emission scanning electron microscope (FESEM) (Carl Zeiss). The particle size distribution of AT powder was measured using a particle size analyzer (Mastersizer 2000, Malvern instruments) based on laser diffraction.

Nickel sulphamate plating bath with the following formulation was used: 300 g  $\text{L}^{-1}$  of nickel sulphamate solution (50 g of nickel per litre), 10 g  $\text{L}^{-1}$  of nickel chloride, 30 g  $\text{L}^{-1}$  of boric acid and 0.2 g  $\text{L}^{-1}$  of sodium lauryl sulphate. The Ni-sulphamate plating bath ( $\sim 200$  mL) containing physically mixed 20 g of AT powder corresponding to 100 g  $\text{L}^{-1}$  (optimised concentration) in a glass beaker was held at room temperature, and its pH was maintained at 4. A pure nickel sheet ( $2.5 \text{ cm} \times 12 \text{ cm}$ ) and a brass substrate of the same dimension were used as anode and cathode respectively. A polished brass substrate with an area of  $2.5(3.75 \text{ cm}^2)$  was degreased with acetone followed by cathodic cleaning, acid dipping and rinsing in distilled water. The electrolyte bath containing particles was subjected to magnetic stirring ( $\sim 600 \text{ rev min}^{-1}$ ) for 15 h before the deposition process to ensure better dispersion. During electrodeposition, the particles were also magnetically stirred at  $600 \text{ rev min}^{-1}$  using a magnetic stirrer with variable rpm (Remi, India). The codeposition was carried out using regulated DC power supply (Aplab 7253) at various current densities:  $0.77 \text{ A dm}^{-2}$  for 6 h,  $1.55 \text{ A dm}^{-2}$  for 3 h,  $3.1 \text{ A dm}^{-2}$  for 1.5 h and  $5.4 \text{ A dm}^{-2}$  for 45 min to get a thickness of  $\sim 50 \mu\text{m}$ . The obtained coatings are hereinafter referred to as Ni/AT.

### X-ray diffraction and microstructural studies of Ni/AT composite coatings

The XRD patterns of plain Ni and Ni/AT composite coatings electrodeposited at  $0.77 \text{ A dm}^{-2}$  were recorded using XRD (Bruker D-8 Advance). The coatings were given a copper backup and then held in an epoxy matrix and subjected to mechanical grinding and polishing with  $\text{Al}_2\text{O}_3$  slurry. The optical micrographs of the cross-sections of Ni/AT coatings were recorded using a vertical metallurgical microscope. The area fraction of particles incorporated in the Ni matrix was calculated from the cross-sectional optical micrographs using image analysis software (Videopro 32).

### Microhardness, wear and corrosion studies

The microhardness of Ni and Ni/AT coatings was measured on 10 different locations on the cross-section of each coating (Micromet 2103, Buehler, 50 gf load). The tribological performance of Ni/AT composite coating electrodeposited at  $0.77 \text{ A dm}^{-2}$  for 8 h was investigated by conducting wear tests on a pin on disc tribometer (DUCOM, India) under ambient conditions of temperature and humidity ( $30^\circ\text{C}$ , 50% RH) at an applied load of 9.8 N. Wear experiments were undertaken for a minimum of three specimens in semicircular

brass pins of radius 6 mm coated with Ni and Ni/AT coatings. The wear tests were conducted at a wear track radius of 30 mm and  $200 \text{ rev min}^{-1}$  (slide speed of  $0.628 \text{ m s}^{-1}$ ) to get a constant sliding distance of 4525 m. The disc used was hardened EN 31 steel with a Vickers hardness of 750 HV. Corrosion behaviour of electrodeposited Ni and Ni/AT coatings electrodeposited at  $0.77 \text{ A dm}^{-2}$  for 2 h on mild steel coupons in 3.5 wt-%NaCl solution was conducted using CHI 604 2D electrochemical workstation. More details regarding the wear and corrosion testing are reported.<sup>15,16</sup> The wear and corrosion results are compared to the reported Ni/ $\text{TiO}_2$  and Ni/ $\text{Al}_2\text{O}_3$  coatings.

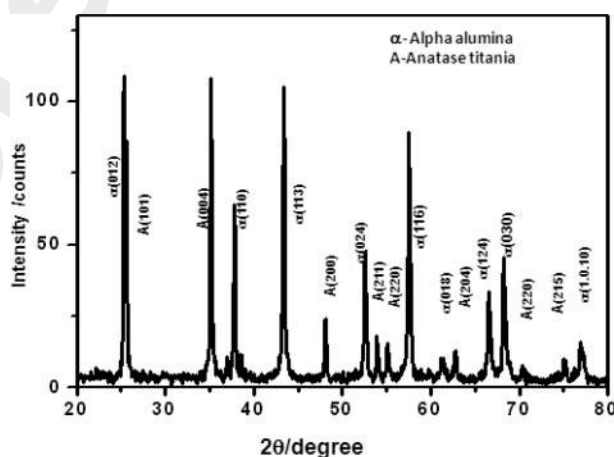
## Results and discussion

### Powder characterization

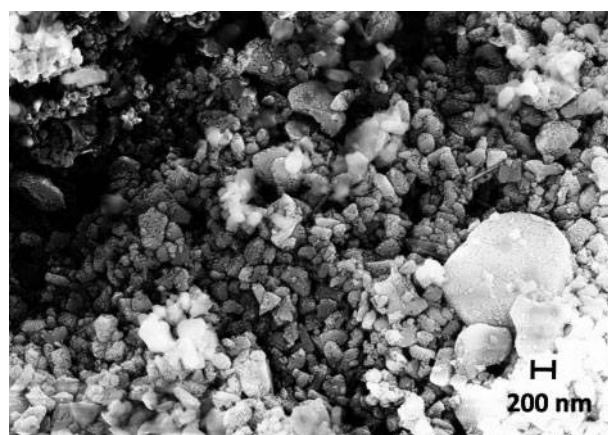
Figure 1 shows the powder XRD pattern of AT powder. From the figure, it is clear that it consists of a mixture of  $\alpha$ -alumina (JCPDS card no. 10-173) and anatase titania (JCPDS card no. 4-0477) phases. Figure 2 shows the FESEM image of AT powder. It shows unagglomerated smaller sized particles. From the particle size distribution, the average agglomerated particle size of AT powder was found to be  $2.4 \mu\text{m}$ .

### X-ray diffraction of Ni/AT coatings

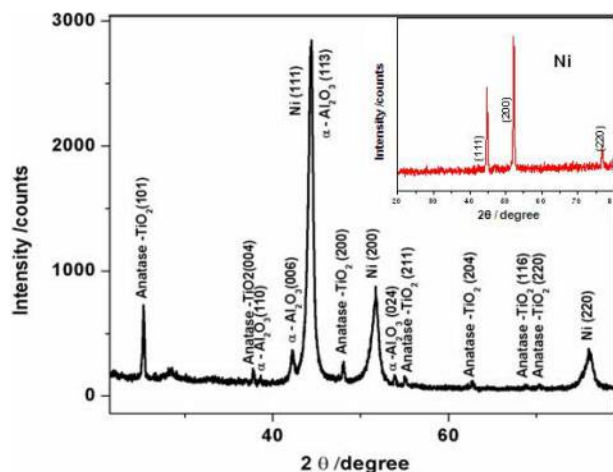
Figure 3 shows the XRD patterns of Ni/AT and Ni (inset) coatings electrodeposited at  $0.77 \text{ A dm}^{-2}$ .



1 Powder XRD pattern of  $\text{Al}_2\text{O}_3$ -13 wt-% $\text{TiO}_2$  (AT) powder

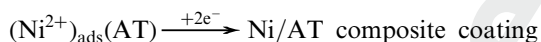


2 Field emission SEM image of AT powder



3 X-ray diffraction patterns of electrodeposited Ni (inset) and Ni/AT coatings

The Ni/AT coating showed the presence of anatase-TiO<sub>2</sub> (JCPDS card no. 4-0477) and α-Al<sub>2</sub>O<sub>3</sub> (JCPDS card no. 10-173) peaks along with Ni (JCPDS card no. 4-0850) peaks. This indicates the incorporation of large number of particles in the Ni matrix. A large number of theoretical models have been proposed by many authors to explain the codeposition of particles in the metal matrix composites. According to the model by Celis,<sup>21</sup> codeposition takes place in five steps: (i) formation of ionic cloud around the particles; (ii) mass transfer of particles by convection to the hydrodynamic layer; (iii) mass transfer of particles to the cathode surface by diffusion; (iv) adsorption of free ions and electroactive ions adsorbed on the particles on the cathode and (v) electroreduction of adsorbed ions accompanied with incorporation of particles into the growing metal matrix. The codeposition of AT particles in Ni matrix can be represented by the following equation



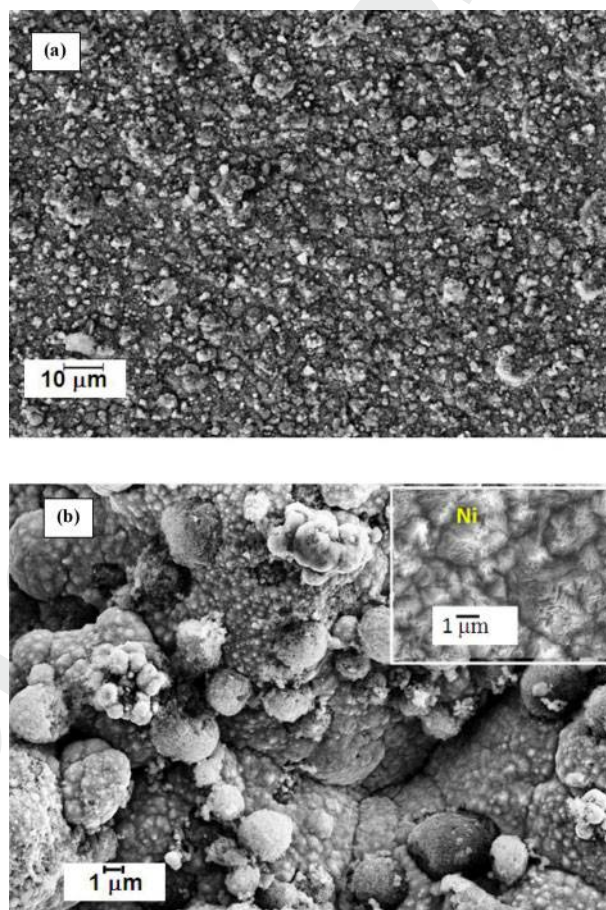
With the incorporation of AT powder in the Ni matrix, the nickel peaks became broader, and a change in the preferred orientation of Ni from (200) to (111) was noticed. The Ni crystallite sizes calculated from Scherrer formula for Ni and Ni/AT coatings were respectively 31 and 16 nm. This may be attributed to the propensity of the particles to preferentially catalyse the reduction in H<sup>+</sup> leading to the inhibition of nickel crystal growth due to the reduction and adsorption of protons from the bulk solution onto the metal surface.<sup>22</sup> In addition, the presence of more particles means that there are more nucleation sites for Ni electrodeposition, and as a result, smaller crystals are formed.

### Microstructure and microhardness of Ni/AT composite coating

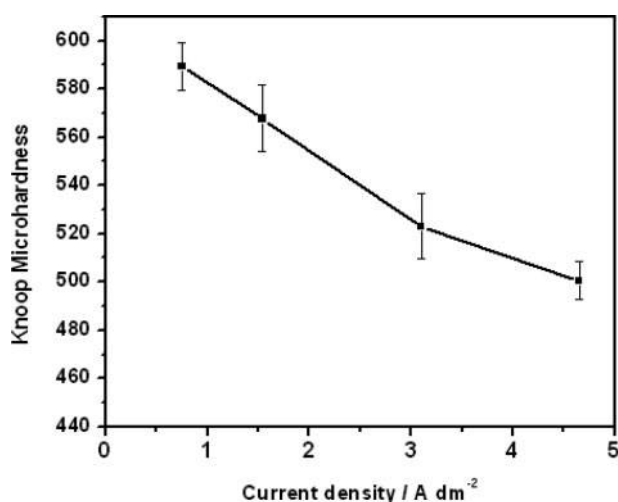
Figure 4 shows the surface FESEM images of Ni/AT coating electrodeposited at 0.77 Adm<sup>-2</sup>. An assessment of the microstructure of the coating surfaces shows that with the incorporation of Al<sub>2</sub>O<sub>3</sub>-TiO<sub>2</sub> powder, there was slight change in the microstructure of the nickel coating; it exhibited nodular structure decorated with particles. The microstructure of plain nickel coating (inset of Fig. 4b) showed irregular pyramidal structure. Energy

dispersive X-ray analysis of the surface of Ni/AT coating showed Al-16.90 wt-%, Ti-2.07 wt-%, Ni-68.97 wt-% and O-12.06 wt-%, confirming the incorporation of large number of alumina and titania particles.

The plots of microhardness versus the current density for Ni-AT coatings are shown in Fig. 5. From the plots, it is seen that higher hardness was observed for coating electrodeposited at lower current density. This may be attributed to the more rapid deposition of metallic cations compared to particle incorporation at higher



4 Field emission SEM images of a,b surface of Ni/AT coating, and inset of b shows FESEM image of plain Ni coating



5 Plots of knoop microhardness versus applied current density of Ni/AT coatings

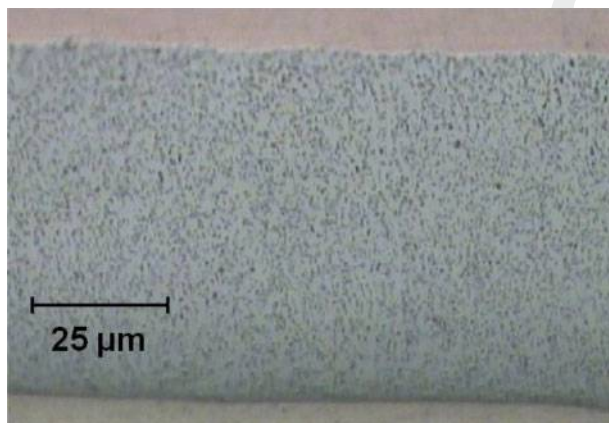


current density. A maximum microhardness of  $\sim 590$  HK was observed for Ni/AT coating electrodeposited at  $0.77 \text{ Adm}^{-2}$ . This value is higher than that reported for Ni/ $\text{Al}_2\text{O}_3$  and Ni/ $\text{TiO}_2$  coatings.<sup>15,16</sup> The observed higher hardness of Ni/AT coating is due to the presence of large number of particles in the coating. Generally, the mechanisms of strengthening of alloys and polycrystalline metals can be described as follows: (i) grain refinement strengthening from Hall–Petch relationship; (ii) dispersion strengthening due to Orowan mechanism; (iii) solid solution strengthening and (iv) crystal orientation.<sup>23</sup> The cross-sectional image of Ni/AT coating (Fig. 6) electrodeposited at  $0.77 \text{ Adm}^{-2}$  exhibited large numbers of particles with an area fraction of 38%. This coating was further analyzed for wear and corrosion resistant properties.

## Wear and corrosion resistant properties of Ni–AT coatings

The wear data of Ni/AT coating are compared with the reported wear data of Ni, Ni/ $\text{Al}_2\text{O}_3$  and Ni/ $\text{TiO}_2$  coatings,<sup>15,16</sup> and the data are tabulated in Table 1. It can be seen from the wear data that Ni/AT coating exhibited a lower coefficient of friction compared to Ni/ $\text{Al}_2\text{O}_3$  due to the presence of softer anatase titania particles. The wear rate of Ni/AT coating was one order of magnitude lower than Ni/ $\text{Al}_2\text{O}_3$  and one order of magnitude higher than Ni/ $\text{TiO}_2$  coatings. Lower the wear rate, higher will be the wear resistance of the coating. Thus, the synergistic effect of alumina and titania particles with respect to the coefficient of friction and wear rate of Ni/AT coating.

The potentiodynamic polarization and electrochemical impedance spectroscopy (EIS) data of Ni,



6 Cross-sectional optical micrograph of Ni/AT coating electrodeposited at  $0.77 \text{ A dm}^{-2}$

Table 1 Comparative wear properties of Ni, Ni/ $\text{Al}_2\text{O}_3$ , Ni/ $\text{TiO}_2$  and Ni/AT coatings

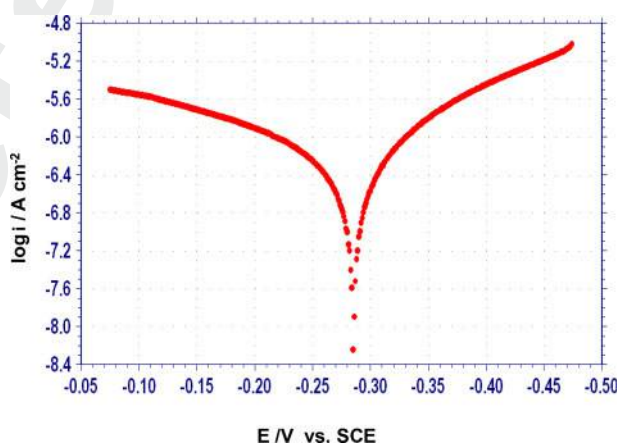
Coating	Average coefficient of friction	Wear volume loss/ $\text{mm}^3$	Wear rate/ $\text{mm}^3 \text{ m}^{-1}$
Pure Ni	0.789	0.1264	$5.59 \times 10^{-5}$
Ni/AT	0.592	0.0035	$1.56 \times 10^{-6}$
Ni/ $\text{Al}_2\text{O}_3$	0.764	0.0799	$2.24 \times 10^{-4}$
Ni/ $\text{TiO}_2$	0.363	0.000678	$2.99 \times 10^{-7}$

Ni/AT and Ni/ $\text{TiO}_2$  coatings are listed in Table 2. The Tafel plot of Ni/AT coating is shown in Fig. 7. It shows smooth curves indicating that the surface is more passive for corrosion attack. The corrosion current density is an important parameter used for evaluating the kinetics of the corrosion reaction as corrosion protection is inversely proportional to the corrosion current density. The corrosion current density for the Ni/AT coating was lower than Ni, which indicates superior corrosion resistance of the coating. It is interesting to note that the potentiodynamic polarization and EIS data matches very well with that reported for Ni/ $\text{TiO}_2$  coating electrodeposited under similar conditions and using same source of particles.<sup>16</sup> However, a comparison of the corrosion data of Ni/AT was not possible with Ni/ $\text{Al}_2\text{O}_3$  as the measurements reported in the literature were carried out with a different instrument.

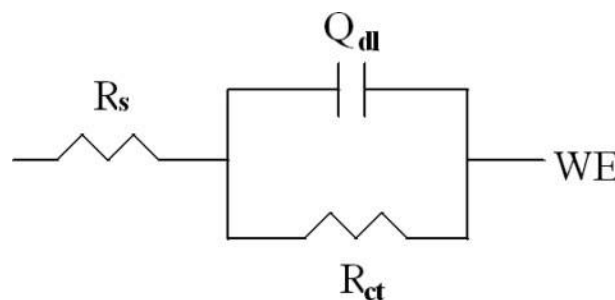
The simple Randles circuit described as R(QR) (Fig. 8) was used for fitting the plots obtained for the Ni/AT

Table 2 Potentiodynamic polarization and EIS results of Ni and Ni/AT composite coatings

Sample	$i_{\text{corr}}/\mu\text{A cm}^{-2}$	$R_p/\text{k}\Omega \text{ cm}^2$	$R_s/\Omega \text{ cm}^2$	$Q_{\text{dl}}-Y_0/(\text{F cm}^{-2})$	$n_{\text{dl}}$	$R_{\text{ct}}/\text{k}\Omega \text{ cm}^2$
Ni	3.608	8.3	1.05	226.1	0.83	7.03
Ni/AT	0.690	56	1.09	33.64	0.93	67.71
Ni/ $\text{TiO}_2$	0.69	56	1.02	36.00	0.91	63.80



7 Tafel plot for Ni/AT coating electrodeposited at  $0.77 \text{ A dm}^{-2}$



8 Equivalent circuit used for Ni and Ni/AT coatings ( $R_s$  – solution resistance of test electrolyte between working electrode and reference electrode,  $Q_{\text{dl}}$  – double layer capacitance,  $R_{\text{ct}}$  – charge transfer resistance and WE – working electrode)

coating, and the fitted values are displayed in Table 2. Figure 9 shows the Nyquist impedance plot of Ni/AT coating. The shape of the impedance spectra describes the type of electrochemical reactions taking place on the electrode surface. Figure 10 shows the Bode plot of Ni/AT composite, and it displayed a single broad peak indicating the large capacitive behaviour of this coating compared to Ni coating. The coatings exhibited phase angle close to  $90^\circ$ , which was reflected in higher  $n$  value. The higher  $R_{ct}$  value for Ni/AT coating indicates that the active area available for corrosive attack is less in this coating. The capacitance  $C$  is represented by a general diffusion related element  $Q$ , which is defined as a constant phase element accounting for the deviation from the ideal dielectric behaviour and is related to surface inhomogeneity. From the Table 2, it is evident that  $Qdl$  value is low for Ni/AT compared to Ni, indicating an improved surface morphology and minimal surface defects compared to Ni. The observed high values of  $R_{ct}$  and low values of  $Qdl$  for Ni/AT coating imply a better corrosion protective ability of this coating compared to plain Ni and Ni/TiO<sub>2</sub> coatings. The reason for improvement of corrosion resistance of Ni-AT can be explained by two mechanisms<sup>24</sup>: (i) AT particles act as inert physical barrier and they inhibit both start and progress of corrosion; and (ii) oxides act as cathode, and metal matrix acts as anode, and since particles have higher inert potential than that of nickel matrix, the localized corrosion is

inhibited and homogeneous corrosion occurs due to the formation of micro galvanic cells.<sup>24</sup>

## Conclusions

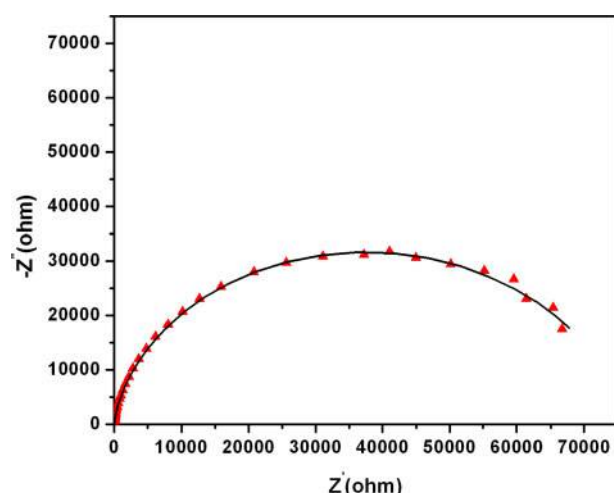
1. In the present study, Al<sub>2</sub>O<sub>3</sub>-13 wt-%TiO<sub>2</sub> (AT) particles were reinforced in nickel matrix by electrodeposition.
2. Ni/AT coating exhibited higher microhardness compared to plain Ni and Ni/TiO<sub>2</sub> coating.
3. Ni/AT coating exhibited higher corrosion resistance compared to Ni coating. The corrosion resistance of Ni/AT was similar to that of Ni/TiO<sub>2</sub>.
4. The coefficient of friction and the wear rate of Ni/AT were in between Ni/Al<sub>2</sub>O<sub>3</sub> and Ni/TiO<sub>2</sub> coatings, and thus, the composite exhibited the synergistic effect of alumina and titania particles.
5. AT powder is a promising candidate material as a reinforcement phase in metal matrix electro-composites for increasing the microhardness, wear and corrosion resistances.

## Acknowledgements

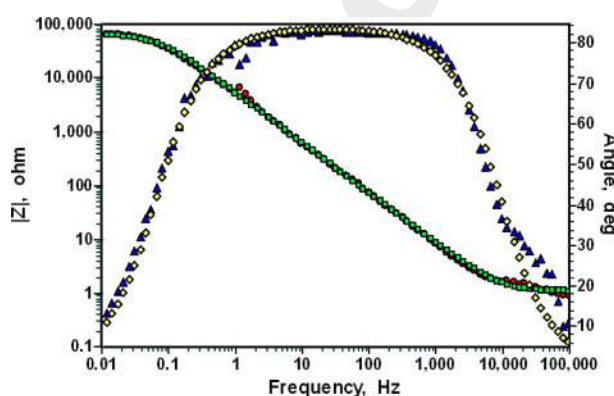
The authors thank Director NAL for his constant encouragement. The authors acknowledge the financial assistance received from the project SIP-SED-02. The authors also thank G. Savitha, S. Latha, Jyothi, M. Prakash and Siju for the help received in electrodeposition, particle size analysis, microhardness, corrosion testing, wear testing and FESEM studies respectively. The authors specially thank Mr V. K. William Grips for useful discussions and suggestions.

## References

1. I. Garcia, J. Fransaer and J.-P. Celis: 'Electrodeposition and sliding wear resistance of nickel composite coatings containing micron and submicron SiC particles', *Surf. Coat. Technol.*, 2001, **148**, 171–178.
2. D. S. Rickerby and A. Matthews: 'Advanced surface coatings: a handbook of surface engineering', 1991, Glasgow, Blackie.
3. J. K. Dennis and T. E. Such: 'Nickel and chromium plating', 3rd edn; 1993, Woodhead Publishing.
4. Hachemi Ben Temam, Abdelouahed Chala and Saâd Rahmane: 'Microhardness and corrosion behavior of Ni-SiC electrodeposited coatings in presence of organic additives', *Surf. Coat. Technol.*, 2011, **205**, (2), S161–S164.
5. S. T. Aruna, C. N. Bindu, V. Ezhil Selvi, V. K. William Grips and K. S. Rajam: 'Synthesis and properties of electrodeposited Ni/ceria nanocomposite coatings', *Surf. Coat. Technol.*, 2006, **200**, 6871–6880.
6. J. M. Li, J. Y. Yin, C. Cai, Z. Zhang, J. F. Li, J. F. Yang, M. Z. Xue and Y. G. Liu: 'Corrosion behavior of nanostructured Ni-Si<sub>3</sub>N<sub>4</sub> composite films: a study of electrochemical impedance spectroscopy', *Mater. Corros.*, 2011, **62**, 9999.
7. M. Raja, G. N. K. Ramesh Babu, J. Maharaja and R. Sekar: 'Electrodeposition and characterisation of Ni-TiC nanocomposite using Watts bath', *Surf. Eng.*, 2014, **30**, 697–701.
8. C. Zanella, M. Lekka and P. L. Bonora: 'Effect of ultrasound vibration during electrodeposition of Ni-SiC nanocomposite coatings', *Surf. Eng.*, 2010, **26**, (7), 511–518.
9. B. L. Bates, L. Z. Zhang and Y. Zhang: 'Electrodeposition of Ni matrix composite coatings with embedded CrAlY particles', *Surf. Eng.*, 2014, **31**, (3), 202–208.
10. J. M. Huang, Y. Li, G. F. Zhang, X. D. Hou and D. W. Deng: 'Electroplating of Ni-ZrO<sub>2</sub> nanocomposite coatings on 40CrNiMo7 alloy', *Surf. Eng.*, 2013, **29**, (3), 194–199.
11. W. Wang, F. -Y. Hou, H. Wang and H. -T. Guo: 'Fabrication and characterization of Ni-ZrO<sub>2</sub> composite nano-coatings by pulse electrodeposition', *Scr. Mater.*, 2005, **53**, 613–618.
12. J. Li, Y. Sun, X. Sun and J. Qiao: 'Mechanical and corrosion-resistance performance of electrodeposited titania-nickel nanocomposite coatings', *Surf. Coat. Technol.*, 2005, **192**, 331–335.



9 Nyquist plot of Ni/AT coating electrodeposited at  $0.77 \text{ A dm}^{-2}$  ( $\blacktriangle$ -measured, and black line simulated)



10 Bode plot of Ni/AT coating electrodeposited at  $0.77 \text{ A dm}^{-2}$  ( $\circ$ - $|Z|$  measured;  $\blacksquare$   $|Z|$  simulated;  $\blacktriangle$  phase angle measured;  $\blacklozenge$  phase angle simulated).

13. P. Bagheri, M. Farzam and M. Hosseini: 'Ni-TiO<sub>2</sub> nanocomposite coating with high resistance to corrosion and wear', *Surf. Coat. Technol.*, 2010, **204**, 3804–3810.
14. X. J. Sun and J. G. Li: 'Friction and wear properties of electrodeposited nickel-titania nanocomposite coatings', *Tribol. Lett.*, 2007, **28**, 223–228.
15. S. T. Aruna, V. Ezhil Selvi, V. K. William Grips and K. S. Rajam: 'Corrosion and wear resistant properties of Ni-Al<sub>2</sub>O<sub>3</sub> composite coatings containing various forms of alumina', *J. Appl. Electrochem.*, 2011, **41**, 461–468.
16. S. T. Aruna, M. Muniprakash and V. K. William Grips: 'Effect of titania particles preparation on the properties of Ni-TiO<sub>2</sub> electrodeposited composite coatings', *J. Appl. Electrochem.*, 2013, **43**, 805–815.
17. F. B. Szczygiel and M. Kolodziej: 'Composite Ni/Al<sub>2</sub>O<sub>3</sub> coatings and their corrosion resistance', *Electrochim. Acta.*, 2005, **50**, 4188–4195.
18. Q. Feng, T. Li, Z. Zhang, J. Zhang, M. Liu and J. Jin: 'Preparation of nanostructured Ni/Al<sub>2</sub>O<sub>3</sub> composite coatings in high magnetic field', *Surf. Coat. Technol.*, 2007, **201**, 6247–6252.
19. R. B. Heimann: 'Application of plasma-sprayed ceramic coatings', *Key Eng. Mater.*, 1996, **399**, 122–124.
20. J. Zhang, J. He, Y. Dong, X. Li and D. Yan: 'Microstructure characteristics of Al<sub>2</sub>O<sub>3</sub>-13 wt.% TiO<sub>2</sub> coating plasma spray deposited with nanocrystalline powders', *J. Mater. Process. Technol.*, 2008, **197**, 31–35.
21. J. P. Celis and J. R. Roos: 'A mathematical model for the electrolytic codeposition of particles with a metallic matrix', *J. Electrochem. Soc.*, 1987, **134**, 1402–1408.
22. B. Watson: 'Electrochemical study of SiC particles occlusion during nickel electrodeposition', *J. Electrochem. Soc.*, 1993, **140**, 2235–2238.
23. H. Gül, F. Kilic, M. Uysal, S. Aslan, A. Alp and H. Akbulut: 'Effect of particle concentration on the structure and tribological properties of submicron particle SiC reinforced Ni metal matrix composite (MMC) coatings produced by electrodeposition', *Appl. Surf. Sci.*, 2012, **258**, 4260–4267.
24. P. Bagheri, M. Farzam, A. B. Mouavi and M. Hosseini: 'Ni-TiO<sub>2</sub> nanocomposite coating with high resistance to corrosion and wear', *Surf. Coat. Technol.*, 2010, **204**, 3804–3810.